

## Explaining the Hubble tension and dark energy from $\alpha$ -attractors

---

**Lucy Brissenden, Konstantinos Dimopoulos\* and Samuel Sánchez López**

*Consortium for Fundamental Physics, Lancaster University,  
Lancaster LA1 4YB, UK*

*E-mail: [l.brissenden@lancaster.ac.uk](mailto:l.brissenden@lancaster.ac.uk), [k.dimopoulos1@lancaster.ac.uk](mailto:k.dimopoulos1@lancaster.ac.uk),  
[s.sanchezlopez@lancaster.ac.uk](mailto:s.sanchezlopez@lancaster.ac.uk)*

A compelling unified model of dark energy and early dark energy (EDE) is presented, using a scalar field with an exponential runaway potential, in the context of alpha-attractors. The field is originally trapped at an enhanced symmetry point, subsequently thaws to become successful EDE and eventually slow-rolls to become dark energy. EDE ameliorates the observed Hubble tension.

*Corfu Summer Institute 2022 "School and Workshops on Elementary Particle Physics and Gravity",  
28 August - 1 October, 2022  
Corfu, Greece*

---

\*Speaker

## 1. Introduction

Since the arrival of high precision cosmological observations, a standard model of cosmology, called the concordance model, has been constructed. In short called  $\Lambda$ CDM, this concordance model recently has starting to suffer from a number of challenges, the most important of which is arguably the Hubble tension.

In a nutshell, the Hubble tension amounts to a disagreement in the estimate of the Hubble constant  $H_0$  as inferred by early (mainly CMB) and late (mainly SNe) observations. Indeed, CMB observations from the Planck satellite [1] suggest

$$H_0 = 67.44 \pm 0.58 \text{ km s}^{-1}\text{Mpc}^{-1}, \quad (1)$$

while a distance scale measurement using Cepheid-SN-Ia data from the SH0ES collaboration [2] results in

$$H_0 = 73.04 \pm 1.04 \text{ km s}^{-1}\text{Mpc}^{-1}. \quad (2)$$

This is a  $5\sigma$  tension ( $4.56$ - $6.36\sigma$ ). The most compelling proposal to overcome this problem is early dark energy (EDE).

## 2. Early Dark Energy

EDE amounts to momentary importance of dark energy near matter-radiation equality. Investigated first by Refs. [3–6], this proposal does not necessarily consider that EDE is the same dark energy substance which is responsible for the accelerated expansion at present (for a recent review see Ref. [7]).

How does EDE manage to increase the value of  $H_0$  as inferred from CMB observations? Even though CMB and BAO observations tightly constrain the cosmological parameters, they constrain the combination  $H(z)r_s$ , where  $H(z)$  is the Hubble parameter as a function of redshift  $z$ , and  $r_s$  is the comoving sound horizon at decoupling, given by

$$r_s = \int_{z_{\text{dec}}}^{\infty} \frac{c_s(z)}{H(z)} dz, \quad (3)$$

where  $c_s(z)$  is the sound speed. An additional amount of dark energy in the Universe increases the total density, which in turn increases the Hubble parameter because of the Friedmann equation  $H^2 = (\rho_B + \rho_{\text{EDE}})/3m_{\text{mp}}^2$ , where  $\rho_B$  is the density of the radiation and matter background. EDE amounts to a brief increase of  $H(z)$  before decoupling, which lowers the value of the sound horizon in Eq. (3). Thus, EDE manages to simultaneously lower the value of  $r_s$  and increase  $H_0$  without violating CMB observations.

The fractional energy density required for EDE to work is about 10%,  $f_{\text{EDE}} = 0.10 \pm 0.02$  at redshift  $z_c = 4070_{-840}^{+400}$ . Therefore, the EDE proposal amounts to as injection of energy at around the time of matter-radiation equality ( $z_c \simeq z_{\text{eq}} \simeq 3600$ ), which then decays away faster than the background radiation, such that it becomes negligible at the time of last scattering, before it can be detected in the CMB [4].

The original proposal in Ref. [3] suggested that the EDE was an axion scalar field  $\phi = \theta f$  with potential  $V(\theta) = m^2 f^2 (1 - \cos \theta)^n$  with  $n > 2$ . The authors of Ref. [3] found that the fractional

energy density must be  $f_{\text{EDE}} = 0.08 \pm 0.04$ , which results in  $H_0 = 70.0 \pm 1.5 \text{ km s}^{-1} \text{ Mpc}^{-1}$ . After thawing, the EDE field oscillates around its vacuum expectation value (VEV) with average barotropic parameter  $w = \frac{n-1}{n+1}$ . To redshift faster than radiation, it is needed that  $w > \frac{1}{3}$ , which implies that the minimum is of order higher than quartic. Note that the density of the oscillating EDE redshifts as  $a^{-6n/(n+1)}$ , which reduces to  $a^{-6}$  (free-fall) in the limit  $n \gg 1$ . The situation is similar to many other EDE models, where typically the EDE scalar field oscillates around its VEV in a high order potential (see however, Ref. [8]). In contrast, in our model presented below, the EDE scalar field experiences a period of kinetic domination, where the field is in non-oscillatory free-fall and its density decreases as  $\propto a^{-6}$ .

### 3. $\alpha$ -attractors

Our model unifies EDE with late dark energy in the context of  $\alpha$ -attractors. Ref. [9] is an earlier attempt for such unification in the same theoretical context. However, that proposal is also of oscillatory EDE.

$\alpha$ -attractors appear naturally in conformal field theory or supergravity theories [10–13]. The scalar field has a non-canonical kinetic term, featuring two poles, which the field cannot cross. The field can be canonically normalised via a field redefinition. Then, the finite poles for the non-canonical field are transposed to infinity for the canonical one. As a result, the scalar potential is “stretched” near the poles, featuring two plateau regions, which have been used for modelling inflation, see *e.g.* Refs. [14–20] or quintessence [21], or both, in the context of quintessential inflation [21–23].

The Lagrangian density features two poles at  $\varphi = \pm\sqrt{6\alpha} m_{\text{P}}$  and has the form

$$\mathcal{L} = \frac{-\frac{1}{2}(\partial\varphi)^2}{\left(1 - \frac{\varphi^2}{6\alpha m_{\text{P}}^2}\right)^2} - V(\varphi), \quad (4)$$

where  $\varphi$  is the non-canonical scalar field and  $(\partial\varphi)^2 \equiv g^{\mu\nu} \partial_\mu\varphi \partial_\nu\varphi$ . Redefining  $\varphi$  in terms of the canonical scalar field  $\phi$ , we have

$$d\phi = \frac{d\varphi}{1 - \frac{\varphi^2}{6\alpha m_{\text{P}}^2}} \quad \Rightarrow \quad \varphi = m_{\text{P}}\sqrt{6\alpha} \tanh\left(\frac{\phi}{\sqrt{6\alpha} m_{\text{P}}}\right). \quad (5)$$

The poles  $\varphi = \pm\sqrt{6\alpha} m_{\text{P}}$  are transposed to infinity and the Lagrangian density now reads

$$\mathcal{L} = -\frac{1}{2}(\partial\phi)^2 - V(\phi). \quad (6)$$

### 4. The Model

In contrast to most EDE literature, we investigate non-oscillating EDE. Thus, we require the scalar potential to be steep enough, such that, after equality of matter and radiation, the EDE scalar field becomes dominated by its kinetic energy density and engages in “free-fall” roll. Therefore, we study the following toy-model.

Consider a potential of the form

$$V(\varphi) = V_X \exp(-\lambda e^{\kappa \varphi / m_P}), \quad (7)$$

where  $\alpha, \kappa, \lambda$  are dimensionless model parameters,  $V_X$  is a constant energy density scale and  $\varphi$  is the non-canonical scalar field with kinetic poles given by the typical  $\alpha$ -attractors form with the Lagrangian density in Eq. (4).

To assist our intuition, we switch to the canonically normalised (canonical) scalar field  $\phi$ , using the transformation in Eq. (5). The Lagrangian density is then given by Eq. (6), where the scalar potential is

$$V(\phi) = \exp(\lambda e^{\kappa \sqrt{6\alpha}}) V_\Lambda \exp[-\lambda e^{\kappa \sqrt{6\alpha} \tanh(\phi / \sqrt{6\alpha} m_P)}], \quad (8)$$

where  $V_\Lambda$  is the vacuum density at present related to the model parameters as

$$V_\Lambda \equiv \exp(-\lambda e^{\kappa \sqrt{6\alpha}}) V_X. \quad (9)$$

Note that the model parameter is  $V_X$  and not  $V_\Lambda$ , the latter being generated by  $V_X$  and the remaining model parameters as shown above.

## 5. Analytic study

We are interested in two limits for the potential: matter-radiation equality and the present time. At matter-radiation equality, we consider  $\phi \rightarrow 0$  ( $\varphi \rightarrow 0$ ). In this limit, we have

$$V_{\text{eq}} \simeq \exp[\lambda(e^{\kappa \sqrt{6\alpha}} - 1)] V_\Lambda \exp(-\kappa \lambda \phi_{\text{eq}} / m_P), \quad (10)$$

where the subscript ‘eq’ denotes the time of matter-radiation equality. It is assumed that the field was originally frozen there and at the time of equality in unfreezes (thaws). We discuss and justify this assumption in Sec. 7.

After thawing the field soon rolls towards large values. Today, we consider  $\phi \rightarrow +\infty$  ( $\varphi \rightarrow +\sqrt{6\alpha} m_P$ ). The potential in this limit is

$$V_0 \simeq V_\Lambda \left[ 1 + 2\kappa \lambda e^{\kappa \sqrt{6\alpha}} \sqrt{6\alpha} \exp\left(-\frac{2\phi_0}{\sqrt{6\alpha} m_P}\right) \right], \quad (11)$$

where the subscript ‘0’ denotes the present time. Note that, in this limit, the potential approaches  $V_\Lambda$ , which corresponds to positive vacuum density with  $w = -1$ , as in  $\Lambda$ CDM.

The above approximations describe well the scalar potential near equality and the present time. As explained below, between these regions, the scalar field free-falls and becomes oblivious of the scalar potential.

Let us investigate the evolution of the EDE field. Originally the field is frozen at zero (see Sec. 7). Its energy density is such that it remains frozen there until equality, when it thaws following the appropriate exponential attractor, since  $V_{\text{eq}}$  in Eq. (10) is approximately exponential [24].

For convenience, we assume this is the subdominant attractor, which requires that the strength of the exponential is [25, 26]

$$\kappa \lambda > \sqrt{3}. \quad (12)$$

The subdominant exponential attractor is called the scaling attractor. In the scaling attractor the energy density of the rolling scalar field mimics the dominant background energy density. Thus, the fractional energy density of the field is constant, given by the value [24–26]

$$f_{\text{EDE}} \simeq \frac{3}{(\kappa\lambda)^2} < 1 \quad (13)$$

This provides an estimate of the moment when the originally frozen scalar field, unfreezes and begins rolling down its potential. Before unfreezing  $f_{\text{EDE}}$  is growing, because the background density decreases with the expansion of the Universe, until  $f_{\text{EDE}}$  obtains the above value.

However, after unfreezing, the field soon experiences the full  $\exp(\exp)$  steeper than exponential potential so, it does not follow the subdominant attractor any more but it is dominated by its kinetic energy density only (it free-falls). Then, its density scales as  $\rho_\phi \simeq \frac{1}{2}\dot{\phi}^2 \propto a^{-6}$ , until it refreezes at a larger value  $\phi_0$ . This value is estimated as follows.

In free-fall, the equation of motion is reduced to  $\ddot{\phi} + 3H\dot{\phi} \simeq 0$ , where  $H = 2/3t$  after equality. The solution is

$$\phi(t) = \phi_{\text{eq}} + \frac{C}{t_{\text{eq}}} \left(1 - \frac{t_{\text{eq}}}{t}\right), \quad (14)$$

where  $C$  is an integration constant. From the above, it is straightforward to find that  $\dot{\phi} = Ct^{-2}$ . Thus, at equality we have

$$\begin{aligned} f_{\text{EDE}} &= \frac{\rho_\phi}{\rho} \Big|_{\text{eq}} = \frac{\frac{1}{2}C^2 t_{\text{eq}}^{-4}}{\frac{4}{3}\left(\frac{m_{\text{P}}}{t_{\text{eq}}}\right)^2} = \frac{3}{8} \frac{C^2}{(m_{\text{P}} t_{\text{eq}})^2} \\ \Rightarrow C &= \sqrt{\frac{8}{3} f_{\text{EDE}}} m_{\text{P}} t_{\text{eq}} = \frac{\sqrt{8}}{\kappa\lambda} m_{\text{P}} t_{\text{eq}}, \end{aligned} \quad (15)$$

where we used Eq. (13),  $\rho_\phi \simeq \frac{1}{2}\dot{\phi}^2$  and that  $\rho = 1/6\pi G t^2 = \frac{4}{3}(m_{\text{P}}/t)^2$ . Therefore, the field freezes at the value

$$\phi_0 = \phi_{\text{eq}} + C/t_{\text{eq}} = \phi_{\text{eq}} + \frac{\sqrt{8}}{\kappa\lambda} m_{\text{P}}, \quad (16)$$

where we considered that  $t_{\text{eq}} \ll t_{\text{freeze}} < t_0$ .

Using that  $t_{\text{eq}} \sim 10^4$  y and  $t_0 \sim 10^{10}$  y, we can estimate

$$\frac{V_{\text{eq}}}{V_0} \simeq \frac{f_{\text{EDE}} \rho_{\text{eq}}}{0.7 \rho_0} \simeq \frac{30}{7(\kappa\lambda)^2} \left(\frac{t_0}{t_{\text{eq}}}\right)^2 \simeq \frac{3}{7(\kappa\lambda)^2} \times 10^{13}. \quad (17)$$

Now, from Eqs. (10) and (11) we find

$$\frac{V_{\text{eq}}}{V_0} \simeq \frac{e^{\lambda(e^{\kappa\sqrt{6\alpha}}-1)} \exp(-\kappa\lambda \phi_{\text{eq}}/m_{\text{P}})}{1 + 2\kappa\lambda e^{\kappa\sqrt{6\alpha}} \sqrt{6\alpha} \exp(-2\phi_0/\sqrt{6\alpha} m_{\text{P}})}. \quad (18)$$

Considering that  $\phi_{\text{eq}} \simeq 0$  and Eq. (16), the above can be written as

$$\frac{V_{\text{eq}}}{V_0} \simeq \frac{e^{\lambda(e^{\kappa\sqrt{6\alpha}}-1)}}{1 + 2\kappa\lambda e^{\kappa\sqrt{6\alpha}} \sqrt{6\alpha} e^{-2\sqrt{8}/\kappa\lambda \sqrt{6\alpha}}}. \quad (19)$$

Taking  $f_{\text{EDE}} \simeq 0.1$  as required by EDE, Eq. (13) suggests

$$\kappa\lambda \simeq \sqrt{30}. \quad (20)$$

Combining this with Eq. (17) we obtain

$$e^{\frac{\sqrt{30}}{\kappa}(e^{\kappa\sqrt{6}\alpha}-1)} \sim 10^{12}/7, \quad (21)$$

where we have ignored the 2nd term in the denominator of the right-hand-side of Eq. (19).

From the above we see that,  $\kappa$  is large when  $\alpha$  is small. Taking, as an example,  $\alpha = 0.01$  we obtain  $\kappa \simeq 18$  and  $\lambda \simeq 0.30$  (from Eq. (20)). With these values, the second term in the denominator of the right-hand-side of Eq. (19) is of order unity and not expected to significantly influence our results.

For the selected values, Eq. (16) suggests that the total excursion of the field is

$$\Delta\phi = \phi_0 - \phi_{\text{eq}} = \frac{\sqrt{8}}{\kappa\lambda} m_P \simeq 0.5 m_P, \quad (22)$$

i.e. it is sub-Planckian. A sub-Planckian excursion of the field implies that 5th force considerations are suppressed.

## 6. Numerical investigation

We have thoroughly analysed this model in Ref. [27]. Here, we will present our main results.

We have aimed to obtain a value of  $H_0$  in the window

$$72 \leq \frac{H_0}{\text{km sec}^{-1} \text{Mpc}^{-1}} \leq 74. \quad (23)$$

With this requirement, the parameter space arrived at for our model parameters is

$$\begin{aligned} 0 < \alpha < 0.00071 \\ 0 < \kappa < 700 \\ 0 < \lambda < 0.027, \end{aligned} \quad (24)$$

with  $V_\Lambda = 10^{-120.068} m_P^4$ . We see that the above numbers are reasonable. In particular, the value of  $\kappa \sim 10^2$  implies that the mass scale suppressing the exponent in our model in Eq. (7) is near the scale of grand unification  $m_P/\kappa \sim 10^{16}$  GeV, which is a rather natural scale.

In the above ranges, we find that  $0.015 < f_{\text{EDE}} < 0.107$  at equality, while it becomes lower than  $10^{-3}$  by decoupling; the time the CMB radiation is emitted. The barotropic parameter of dark energy at present is  $w_\phi = -1.000$  with negligible running (less than  $10^{-11}$ ), which is indistinguishable from  $\Lambda$ CDM.

One important finding is that the condition in Eq. (12),  $\kappa\lambda > \sqrt{3}$  assumed in the previous section, is not valid. However, this was chosen only for convenience, as explained before Eq. (12). If the condition is violated then the thawing EDE does not follow the scaling exponential attractor

but the dominant exponential attractor instead. In both cases however, once the EDE field rolls away from zero, it starts experiencing the full  $\exp(\exp)$  potential and goes into free-fall, as discussed. Thus, the qualitative behaviour is the same, as also demonstrated by our numerical results shown below.

As a concrete example, we choose the following values for the model parameters

$$\begin{aligned} \alpha &= 0.0005 \\ \kappa &= 145 \\ \lambda &= 0.008125. \end{aligned} \tag{25}$$

The above suggest that  $\kappa\lambda = 1.178 < \sqrt{3}$ . The value of the Hubble constant obtained in this case is

$$H_0 = 73.27 \text{ km sec}^{-1} \text{ Mpc}^{-1}, \tag{26}$$

which evidently is well in agreement with the SH<sub>0</sub>ES observations. Comparison of the Hubble parameter in this scenario with the one in  $\Lambda$ CDM is shown in Fig. 1.

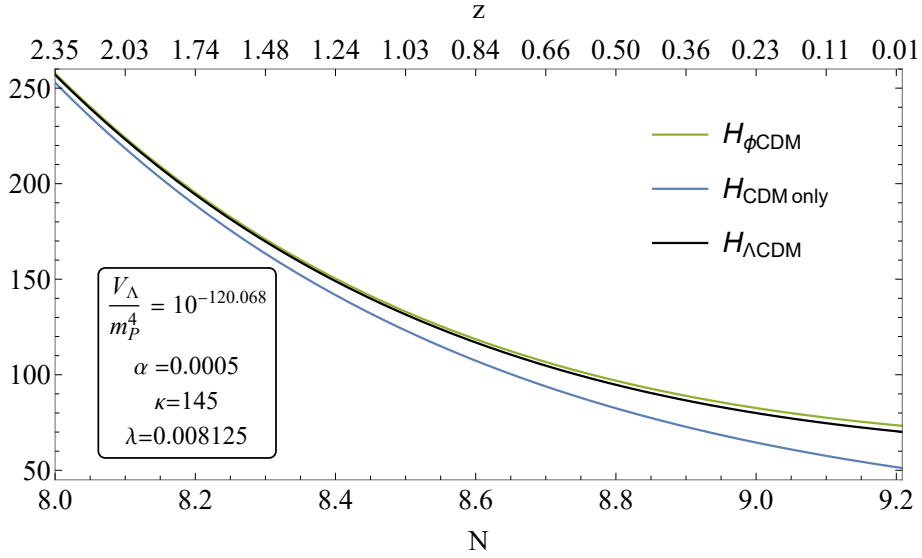


**Figure 1:** The Hubble parameter (in units of  $\text{km s}^{-1}\text{Mpc}^{-1}$ ) of the Universe in our model (green), a classical  $\Lambda$ CDM simulation (black), and one with only matter and radiation (blue), as a function of the redshift (top) and the e-folds (bottom) elapsed since the beginning of the simulation. It is evident that our model corresponds to a larger value of  $H(z)$  than  $\Lambda$ CDM, as desired.

The behaviour of the fractional energy density  $f_{\text{EDE}}$ , which is identified with the EDE density parameter  $\Omega_\phi(z)$  is shown in Fig. 2. It is evident that, for this example,  $f_{\text{EDE}} = \Omega_\phi(z_{\text{eq}}) \simeq 0.08$ .

In view of Eq. (9), we find  $\log(V_X/V_\Lambda) = 9.926$ . Thus, our model parameter  $V_X = 10^{-110.142} m_p^4$  is fine-tuned at the same level (slightly less) than  $V_\Lambda$  in  $\Lambda$ CDM. However, it has to be stressed that, in contrast to  $\Lambda$ CDM, our proposal addresses simultaneously two cosmological problems; not only late dark energy but also the Hubble tension.

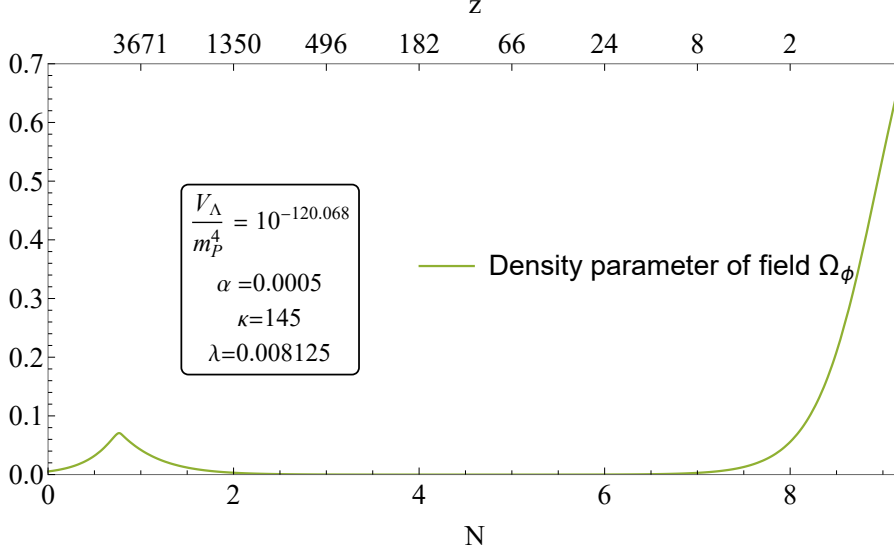


**Figure 2:** The density parameter of the scalar field  $\Omega_\phi$  as a function of the redshift (top) and e-folds (bottom) elapsed since the beginning of the simulation. As shown, at equality, there is a bump with  $f_{\text{EDE}} = \Omega_\phi(z_{\text{eq}})$  with  $f_{\text{EDE}} \simeq 0.08$ .

The barotropic parameters, of EDE and the background, are shown in Fig. 3. It can be seen clearly that, after thawing, the barotropic parameter of EDE is  $w_\phi = 1$  and the field is in free-fall as discussed. Its density decreases as  $a^{-6}$  as clearly shown in Fig. 4, which corresponds to the  $n \rightarrow \infty$  limit of the oscillating EDE in Ref. [3] and it is never attained by any oscillating EDE model. Thus, our model disturbs the emission of the CMB at decoupling in the least amount possible.

Finally, for our example we obtain that the total excursion of the EDE field from thawing to refreezing is sub-Planckian:  $\Delta\phi/m_{\text{P}} = 0.4274$ , in agreement with Eq. (22). This implies both that our model does not suffer from fifth force problems and our potential is stable against radiative corrections.

## 7. Trapping at the origin

A compelling explanation why the EDE scalar field finds itself frozen at the origin in the first place is the following. If the origin is an enhanced symmetry point (ESP), then at very early times, an interaction of  $\varphi$  with some other scalar field  $\sigma$  can trap the rolling  $\varphi$  at zero [28]. The scalar potential includes the interaction

$$\Delta V = \frac{1}{2}g^2\varphi^2\sigma^2, \quad (27)$$

where the coupling  $g < 1$  parametrises the strength of the interaction.

We assume that initially  $\varphi$  is rolling down its steep potential, which away from the origin, does not have to be of the form in Eq. (7). In fact, it is conceivable that  $\varphi$  might play the role of the inflaton field too [27]. The original kinetic energy density of  $\varphi$  is depleted due to particle production of  $\sigma$ -particles, because their mass  $\sim g\varphi$  changes non-adiabatically near the origin [28]. Note that, near the origin, the  $\varphi$ -field is approximately canonically normalised.



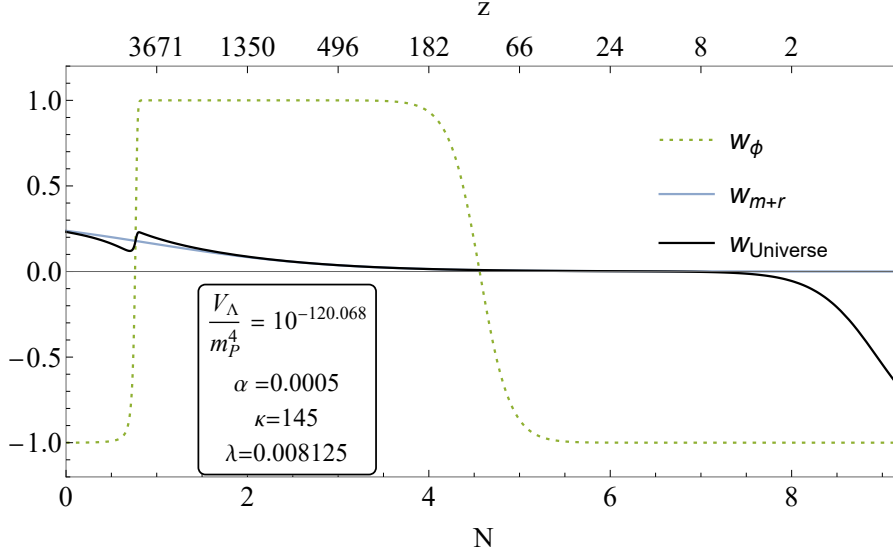


**Figure 3:** Barotropic parameter of the scalar field (dotted green), of the background perfect fluid (full blue) and of the sum of both components (full black). It is evident that, after unfreezing, the EDE scalar field is in free-fall, with  $w_\phi = 1$ , until it refreezes again.

As the field moves past the ESP, the produced  $\sigma$  particles give rise to an effective linear potential  $\sim gn_\sigma|\varphi|$  [28], where  $n_\sigma$  is the number density of the produced  $\sigma$ -particles. This linear potential halts the roll of  $\varphi$  and reverses its variation. More  $\sigma$ -particles are created when  $\varphi$  crosses the origin again, resulting in a steeper linear potential, which reverses the variation of  $\varphi$  again, closer to the origin this time. The process continues until the  $\varphi$ -field is trapped at the origin [26, 28].

The trapping of a rolling scalar field at an ESP can take place only if the  $\sigma$ -particles do not decay at maximum displacement. The end result of this process is that all the kinetic energy density of the rolling  $\varphi$  has been given to the  $\sigma$ -particles. Since  $\varphi$  is trapped at zero, the  $\sigma$ -particles are relativistic, which means that their density scales as radiation, being a subdominant part of the thermal bath. As far as  $\varphi$  is concerned, it is trapped at the origin and its density is  $\rho_\varphi = V(\varphi = 0) = e^{-\lambda}V_X = \text{constant}$ .

After some time, the  $\sigma$ -particles may decay into the standard model particles, which comprise the thermal bath of the hot Big Bang. Because the confining potential is proportional to  $n_\sigma$ , it disappears. However, the EDE  $\varphi$ -field remains frozen at the origin because the scalar potential  $V(\varphi)$  in Eq. (7) is flat enough there. The EDE  $\varphi$ -field unfreezes again in matter-radiation equality.

The above scenario is one possible explanation of the initial condition considered. Numerical simulations simply assume that the field begins frozen at the origin. Other possibilities to explain our initial condition exist, for example considering a thermal correction of the form  $\delta V \propto T^2\varphi^2$ , which would drive the  $\varphi$ -field towards the origin at high temperatures.

## 8. Conclusions

The concordance model  $\Lambda$ CDM suffers from the Hubble tension at  $5\sigma$ . A prominent resolution of this tension is early dark energy (EDE). EDE amounts to a dark energy substance, which

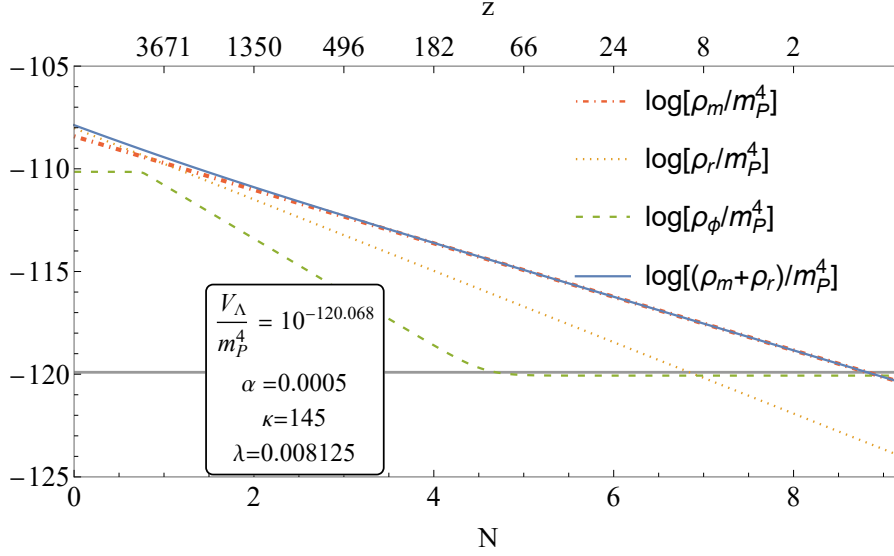


**Figure 4:** The logarithmic densities of matter (dot-dashed red), radiation (dotted orange), the sum of both (solid blue) and the EDE scalar field (dashed green), as a function of the redshift (top) and the e-folds (bottom) elapsed since the beginning of the simulation. The horizontal full line represents the ( $SH_0ES$ ) energy density of the Universe at present. As shown, after it briefly becomes important near equality, the density of EDE scalar field is reducing drastically and it is orders of magnitude smaller than that of the matter background by the time of decoupling ( $z_{\text{dec}} = 1090$ ), as required.

momentarily becomes about 10% of the total energy density near matter-radiation equality, but decays faster than radiation afterwards.

EDE in the context of  $\alpha$ -attractors can unify EDE with late dark energy without more fine-tuning than  $\Lambda$ CDM. We studied such a model of EDE, characterised by the  $\exp(\exp)$  potential in Eq. (7). Our EDE is originally frozen at the origin. Near equality it thaws, then it free-falls down its runaway potential until it refreezes before today, when it becomes late dark energy.

We have investigated numerically our model and demonstrated that it works for natural values of the parameters. We also showed that the field excursion between the initial and final frozen values is sub-Planckian, which means that our model does not suffer from a fifth force problem and it is not unstable against radiative corrections.

**Acknowledgements:** LB is supported by STFC. KD is supported (in part) by the Lancaster-Manchester-Sheffield Consortium for Fundamental Physics under STFC grant: ST/T001038/1. SSL is supported by the FST of Lancaster University. For the purpose of open access, the authors have applied a Creative Commons Attribution (CC BY) licence to any Author Accepted Manuscript version arising.

## References

- [1] N. Aghanim *et al.* [Planck], *Planck 2018 results. VI. Cosmological parameters*, *Astron. Astrophys.* **641** (2020), A6 [erratum: *Astron. Astrophys.* **652** (2021), C4] doi:10.1051/0004-6361/201833910 [arXiv:1807.06209 [astro-ph.CO]].

- [2] A. G. Riess, W. Yuan, L. M. Macri, D. Scolnic, D. Brout, S. Casertano, D. O. Jones, Y. Murakami, L. Breuval and T. G. Brink, *et al. A Comprehensive Measurement of the Local Value of the Hubble Constant with 1 km/s/Mpc . Uncertainty from the Hubble Space Telescope and the SH0ES Team*, *Astrophys. J. Lett.* **934** (2022) no.1, L7 doi:10.3847/2041-8213/ac5c5b [arXiv:2112.04510 [astro-ph.CO]].
- [3] T. Karwal and M. Kamionkowski, *Dark energy at early times, the Hubble parameter, and the string axiverse*, *Phys. Rev. D* **94** (2016) no.10, 103523 doi:10.1103/PhysRevD.94.103523 [arXiv:1608.01309 [astro-ph.CO]].
- [4] V. Pettorino, L. Amendola and C. Wetterich, *How early is early dark energy?*, *Phys. Rev. D* **87** (2013), 083009 doi:10.1103/PhysRevD.87.083009 [arXiv:1301.5279 [astro-ph.CO]].
- [5] E. Calabrese, D. Huterer, E. V. Linder, A. Melchiorri and L. Pagano, *Limits on Dark Radiation, Early Dark Energy, and Relativistic Degrees of Freedom*, *Phys. Rev. D* **83** (2011), 123504 doi:10.1103/PhysRevD.83.123504 [arXiv:1103.4132 [astro-ph.CO]].
- [6] M. Doran and G. Robbers, *Early dark energy cosmologies*, *JCAP* **06** (2006), 026 doi:10.1088/1475-7516/2006/06/026 [arXiv:astro-ph/0601544 [astro-ph]].
- [7] V. Poulin, T. L. Smith and T. Karwal, *The Ups and Downs of Early Dark Energy solutions to the Hubble tension: a review of models, hints and constraints circa 2023*, arXiv:2302.09032 [astro-ph.CO].
- [8] M. X. Lin, G. Benevento, W. Hu and M. Raveri, *Acoustic Dark Energy: Potential Conversion of the Hubble Tension*, *Phys. Rev. D* **100** (2019) no.6, 063542 doi:10.1103/PhysRevD.100.063542 [arXiv:1905.12618 [astro-ph.CO]].
- [9] M. Braglia, W. T. Emond, F. Finelli, A. E. Gumrukcuoglu and K. Koyama, *Unified framework for early dark energy from  $\alpha$ -attractors*, *Phys. Rev. D* **102** (2020) no.8, 083513 doi:10.1103/PhysRevD.102.083513 [arXiv:2005.14053 [astro-ph.CO]].
- [10] R. Kallosh, A. Linde and D. Roest, *Superconformal Inflationary  $\alpha$ -Attractors*, *JHEP* **11** (2013), 198 doi:10.1007/JHEP11(2013)198 [arXiv:1311.0472 [hep-th]].
- [11] R. Kallosh and A. Linde, *Universality Class in Conformal Inflation*, *JCAP* **07** (2013), 002 doi:10.1088/1475-7516/2013/07/002 [arXiv:1306.5220 [hep-th]].
- [12] S. Ferrara, R. Kallosh, A. Linde and M. Porrati, *Minimal Supergravity Models of Inflation*, *Phys. Rev. D* **88** (2013) no.8, 085038 doi:10.1103/PhysRevD.88.085038 [arXiv:1307.7696 [hep-th]].
- [13] R. Kallosh, A. Linde and D. Roest, *Large field inflation and double  $\alpha$ -attractors*, *JHEP* **08** (2014), 052 doi:10.1007/JHEP08(2014)052 [arXiv:1405.3646 [hep-th]].
- [14] A. Alho and C. Uggl, *Inflationary  $\alpha$ -attractor cosmology: A global dynamical systems perspective*, *Phys. Rev. D* **95** (2017) no.8, 083517 doi:10.1103/PhysRevD.95.083517 [arXiv:1702.00306 [gr-qc]].

- [15] S. D. Odintsov and V. K. Oikonomou, *Inflationary  $\alpha$ -attractors from  $F(R)$  gravity*, Phys. Rev. D **94** (2016) no.12, 124026 doi:10.1103/PhysRevD.94.124026 [arXiv:1612.01126 [gr-qc]].
- [16] M. Braglia, A. Linde, R. Kallosh and F. Finelli, *Hybrid  $\alpha$ -attractors, primordial black holes and gravitational wave backgrounds*, [arXiv:2211.14262 [astro-ph.CO]].
- [17] R. Kallosh and A. Linde, *Hybrid cosmological attractors*, Phys. Rev. D **106** (2022) no.2, 023522 doi:10.1103/PhysRevD.106.023522 [arXiv:2204.02425 [hep-th]].
- [18] A. Achúcarro, R. Kallosh, A. Linde, D. G. Wang and Y. Welling, *Universality of multi-field  $\alpha$ -attractors*, JCAP **04** (2018), 028 doi:10.1088/1475-7516/2018/04/028 [arXiv:1711.09478 [hep-th]].
- [19] O. Iarygina, E. I. Sfakianakis, D. G. Wang and A. Achúcarro, *Multi-field inflation and preheating in asymmetric  $\alpha$ -attractors*, [arXiv:2005.00528 [astro-ph.CO]].
- [20] K. Dimopoulos, *Waterfall stiff period can generate observable primordial gravitational waves*, JCAP **10** (2022), 027 doi:10.1088/1475-7516/2022/10/027 [arXiv:2206.02264 [hep-ph]].
- [21] Y. Akrami, R. Kallosh, A. Linde and V. Vardanyan, *Dark energy,  $\alpha$ -attractors, and large-scale structure surveys*, JCAP **06** (2018), 041 doi:10.1088/1475-7516/2018/06/041 [arXiv:1712.09693 [hep-th]].
- [22] K. Dimopoulos, L. Donaldson Wood and C. Owen, *Instant preheating in quintessential inflation with  $\alpha$ -attractors*, Phys. Rev. D **97** (2018) no.6, 063525 doi:10.1103/PhysRevD.97.063525 [arXiv:1712.01760 [astro-ph.CO]].
- [23] K. Dimopoulos and C. Owen, *Quintessential Inflation with  $\alpha$ -attractors*, JCAP **06** (2017), 027 doi:10.1088/1475-7516/2017/06/027 [arXiv:1703.00305 [gr-qc]].
- [24] E. J. Copeland, A. R. Liddle and D. Wands, *Exponential potentials and cosmological scaling solutions*, Phys. Rev. D **57** (1998), 4686-4690 doi:10.1103/PhysRevD.57.4686 [arXiv:gr-qc/9711068 [gr-qc]].
- [25] E. J. Copeland, M. Sami and S. Tsujikawa, *Dynamics of dark energy*, Int. J. Mod. Phys. D **15** (2006), 1753-1936 doi:10.1142/S021827180600942X [arXiv:hep-th/0603057 [hep-th]].
- [26] K. Dimopoulos, *Introduction to Cosmic Inflation and Dark Energy*, CRC Press, 2022, ISBN 978-0-367-61104-0
- [27] L. Brissenden, K. Dimopoulos and S. Sánchez López, *Non-oscillating Early Dark Energy and Quintessence from  $\alpha$ -attractors*, arXiv:2301.03572 [astro-ph.CO].
- [28] L. Kofman, A. D. Linde, X. Liu, A. Maloney, L. McAllister and E. Silverstein, *Beauty is attractive: Moduli trapping at enhanced symmetry points*, JHEP **05** (2004), 030 doi:10.1088/1126-6708/2004/05/030 [arXiv:hep-th/0403001 [hep-th]].